J Mater Sci (2011) 46:3725–3737
DOI 10.1007/s10853-011-5285-2

Effect of deformation temperature on microstructure and mechanical behaviour of warm working vanadium microalloyed steels

C. García-Mateo · B. López · J. M. Rodriguez-Ibabe

Received: 8 July 2010 / Accepted: 20 September 2010 / Published online: 29 January 2011

Abstract Plane strain compression tests of two V microalloyed steels and one plain C–Mn steel have been done to analyse the influence of the deformation temperature, in the warm working range, on the final microstructure and subsequent mechanical behaviour. In the case of V microalloyed steels, the reheating temperature has an effect on the amount of vanadium in solution prior to deformation. This factor influences the austenite evolution during warm deformation and the transformation during cooling. As a consequence, in the microalloyed steels complex multiphase microstructures are obtained that lead to a wide range of strength–toughness combinations. In contrast, in the case of the plain C–Mn steel minor effects are observed in the deformation range from 800 to 870 °C.

Introduction

Nowadays there is a continuous demand, particularly from the automotive industry, for cheaper, lighter and more reliable components and, at the same time, steel is facing strong competition from various other groups of materials in a market that was traditionally its own. It is not surprising that during the last 25 years, the steel industry has experienced some of the most important changes at two different fronts, steel design and processes. Steel manufacturing processes face major competitions in the automotive industry to produce lighter, cheaper and more efficient components that exhibit dimensions that are more precise, need less machining and require less part processing. In that respect, mechanical and metallurgical properties, as well as the manufacturing parameters, play decisive roles [1, 2].

Hot forging grades have been traditionally plain carbon, alloyed and microalloyed steels. Their final mechanical properties are achieved after applying quenching and tempering heat treatments or directly cooling after forging. In all the cases machining operations are required to obtain the final shape and dimensions. It is worth emphasising that the distribution of the costs in producing conventional forging components shows that more than 50% is assigned to machining, besides of the cost of the base material, the forging process and the heat treatment [3]. Taking into account this aspect, a great interest has emerged in the near-net-shape technologies, as cold and warm forging processes. Concerning warm forging (usually in the temperature range from 600 to 900 °C), this route has a number of advantages over traditional forging procedures [4–7]. Among them, the following advantages need to be considered: better utilisation of material, improved surface finish, dimensional accuracy compared with hot forging, reduced press loads compared with cold forging, and control of the microstructure such that the desired properties can be obtained without further heat treatments. The process fills the niche between the closer tolerance, but sometimes expensive, cold forging process and the somewhat lower precision of hot forging route.

The production of warm forged components was initially based on plain carbon steels with final ferrite–pearlite microstructures at room temperature [6]. In the last

C. García-Mateo (✉)
Materalia Research Group, Department of Physical Metallurgy, Centro Nacional de Investigaciones Metalúrgicas (CENIM), Consejo Superior de Investigaciones Científicas (CSIC), Avda. Gregorio del Amo 8, E-28039 Madrid, Spain
e-mail: cgm@cenim.csic.es

B. López · J. M. Rodriguez-Ibabe
CEIT and Tecnun (University of Navarra), P. M. Lardizabal 15, E-20018 San Sebastián, Basque Country, Spain

years, warm forging techniques have also been extended to components based on low alloy steel grades, requiring specific studies concerning flow stress behaviour of these grades in the 600–900 °C temperature range [8, 9]. In a similar way to what happened with conventional forging, the introduction of microalloyed steel grades in warm forging has been considered as an option to obtain better strength–toughness combinations in comparison to plain C–Mn steels. Initially vanadium was considered as the main microalloyed option [5], while more recently Nb microalloying has appeared as a very promising possibility [10, 11].

In the case of hot forging, the introduction of vanadium assigned to this element its conventional role of precipitation strengthening during cooling at the exit of the forging. In contrast, this situation changes significantly in the case of warm forging [12]. It is necessary to take into account that, depending on the reheating temperature prior to warm forming, a fraction of V(C,N) particles present in the as-rolled condition will remain undissolved, while in conventional hot forming all the vanadium is in solution and, as a consequence, available to precipitate during cooling. These undissolved particles can interact with the microstructure in different scenarios. For example, it has been reported that undissolved V(C,N) precipitates can reduce the austenite grain growth during reheating and similarly, they can delay austenite static recrystallisation kinetics after deformation [13, 14]. Both factors can have beneficial effects on final room temperature properties by promoting additional microstructural refinement. In contrast, depending on the reheating temperature the reduced amount of vanadium available to precipitate during cooling can reduce its contribution to precipitation strengthening.

The aim of this work is to study the potential that warm forging in combination with V microalloying may have on the final properties of steels. For this purpose two vanadium microalloyed steel grades and a typical forging C–Mn steel, for comparison, have been used.

Material and experimental procedure

Two commercial vanadium microalloyed steels with different C and V contents and, for the sake of comparison, a plain C–Mn steel were selected for this study. Their chemical compositions are listed in Table 1 content. Warm forging simulations were performed in a servo hydraulic press by testing plane strain compression specimens of $25 \times 60 \times 10$ mm^3, machined from industrially hot rolled steel bars. Specimens were heated in a resistance furnace and soaked at the deformation temperature for 10 min before testing. In order to minimise the effect of friction and temperature gradient profiles, which may lead to inhomogeneities in deformation distribution, samples were lubricated with boron nitride and both, samples and die tools, were kept inside the furnace during all the experiment. Finally, specimens were deformed to a strain of $\varepsilon = 0.3$ at a strain rate of 10 s^{-1}. Following deformation, specimens were subjected to two different cooling rates, i.e., air cooling ($\approx$1 °C/s) and accelerated cooling ($\approx$4 °C/s). Three different testing temperatures were considered 800, 835 and 870 °C, all of them in the austenite range.

Table 1 Chemical composition of the steels examined (wt%)

Steel	C	Mn	Si	Cr	Ni	Mo	Cu	V	N
V1	0.24	1.56	0.28	0.10	0.09	0.04	0.24	0.18	0.010
V2	0.33	1.49	0.25	0.08	0.11	0.04	0.27	0.24	0.010
C–Mn	0.47	0.78	0.24	0.17	0.08	0.02	0.10	0.002	0.009

Prior austenite grain size (PAGS) before deformation was determined metallographically from quenched specimens after soaking at the testing temperature. In order to reveal the PAGS it was necessary to temper the specimens at 450–500 °C for periods in excess of 24 h for V microalloyed steels and 2 h in the case of the plain C–Mn steel, respectively. After the treatment, the samples were polished and etched in a solution of saturated picric acid. Prior austenite grain size was measured by the mean equivalent diameter method.

Microstructural characterisation was carried out using optical and scanning electron microscopy on metallographic samples cut longitudinally from the plane strain compression specimens. Round tensile samples (4 mm diameter and 10 mm gauge length) and V-notch Charpy impact specimens (sub-size samples of 5×10 mm) were machined from plane strain compression specimens. In the case of the Charpy tests, the absorbed energies were converted to standard specimen dimensions [15].

Carbon replicas were prepared by conventional methods, and observed in a transmission electron microscope (TEM) fitted with an energy dispersive X-ray system. The size and distribution of V precipitates were quantified for the different conditions, measuring in each case a minimum of 500 and a maximum of 1200 particles.

MTDATA [16] fitted with NPL-plus database for steels was used to theoretically estimate the amount of V in solid solution and the mass fraction of V precipitates as a function of temperature.

Results

Microstructural characterisation

Figure 1 shows the mean austenite grain size as a function of the reheating temperature. Data corresponding to

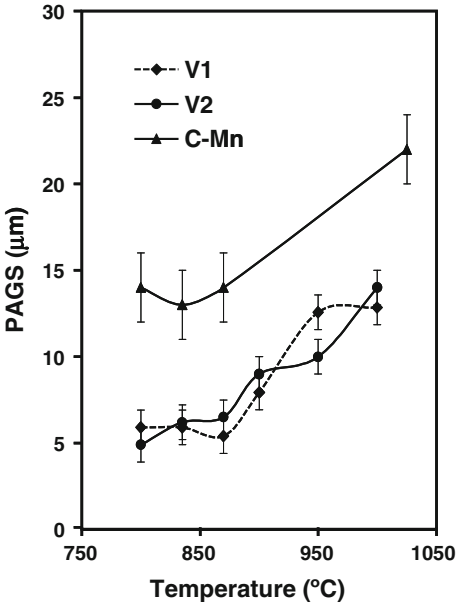

Fig. 1 Austenite grain size evolution with reheating temperature

reheating temperatures higher than initially considered for warm forging conditions (that is, lower than 900 °C) have been included for comparison.

The microstructures of the vanadium microalloyed steels at room temperature consist of a mixture of ferrite, pearlite/bainite and martensite/austenite constituent (MA), as shown in Fig. 2. The pearlite present in these steels has not its normal lamellar structure and can be considered as "degenerated pearlite". Besides this pearlite bainite is also identified although it is difficult, because of the morphology of the pearlite, to distinguish between both constituents. In some regions, mainly in the case of V2 steel, the MA constituents show a banded tendency. In the case of the plain carbon steel, the microstructure is ferrite–pearlite with well-defined lamellar pearlite.

The metallographic measurements of the ferrite mean grain size and ferrite volume fraction are shown in Fig. 3 as a function of the deformation temperature. In both vanadium microalloyed steels, at 800 and 835 °C deformation temperatures the ferrite grain size remains very small with a mean size ranging between 2.1 and 3.4 μm after air cooling. The accelerated cooling does not lead to an additional refinement, in contrast to what happens after deforming at 870 °C. In this later case, the grain sizes are slightly coarser than those measured at the other two conditions. In relation to the plain C–Mn steel the ferrite grain size is coarser that those corresponding to the V microalloyed steels, although it continues being fine.

In relation to the ferrite volume fraction, the results obtained for the three steels are shown in Fig. 3 as a function of deformation temperature and cooling rate. While at 800 and 870 °C the ferrite fraction tends to decrease, regardless of the cooling rate, with the carbon content present in the steel, at 835 some changes in this behaviour have been identified. Thus, at 835 °C in the V2 steel the ferrite content is higher than that measured in steel V1 for both cooling conditions. In all the conditions, the accelerated cooling reduces the ferrite fraction in relation to the air cooled samples. Finally, in the plain C–Mn steel the ferrite fraction remains nearly unaffected by the deformation temperature.

The volume fraction of the MA constituent present in the vanadium microalloyed steels has been drawn in Fig. 4 as a function of the deformation temperature. Increasing the deformation temperature the MA volume fraction increases, ranging from 5% at 800 °C to 18% at 870 °C in the air cooled samples. These values are significantly higher when accelerated cooling is applied. On the other hand, the mean size of the MA constituents slightly increases with the deformation temperature, ranging from 2.0 to 5.5 μm. Nevertheless, the effect of cooling rate is not always the same. For example, while coarser MA constituents appear at 800 °C and accelerated cooling, the opposite occurs at 835 and 870 °C. Comparing both V1 and V2 steels, similar or even coarser sizes have been measured in steel V1 at all the conditions.

Due to the different roles that precipitates can play in both microalloyed steels, an exhaustive analysis of the precipitate size distribution and density formed under different conditions was performed. In the as received condition, the spherical particles observed in both vanadium microalloyed steels were identified as V rich precipitates. The size distribution of these particles is shown in Fig. 5. In the figure, it can be seen that V1 steel exhibits a distribution of very fine precipitates with a mean diameter of 8 nm, 71% of the precipitates being smaller than 9 nm, while in V2 steel the precipitates are slightly coarser with a mean size of 14 nm. The number of particles per area unit (ρ) is also indicated in the figure.

Figure 6 shows the size distribution of V precipitates after reheating for 10 min at 870 and 835 °C followed by water quench. If these results are compared with those of Fig. 5 (as received condition) it is possible to see a displacement of the size distribution towards coarser particle sizes as heating temperature increases. This behaviour denotes that there has been a dissolution process involving, above all, the smallest precipitates, which is also confirmed by the significant decrease in the number of particles per area unit. Finally, the precipitate size distributions after deformation followed by air cooling are shown in Fig. 7 for steel V1 at deformation temperatures of 800 and 870 °C and for steel V2 at a deformation temperature of 870 °C, respectively. Results indicate that deformation at 870 °C induces a refinement in the particle size distribution while lower deformation temperatures

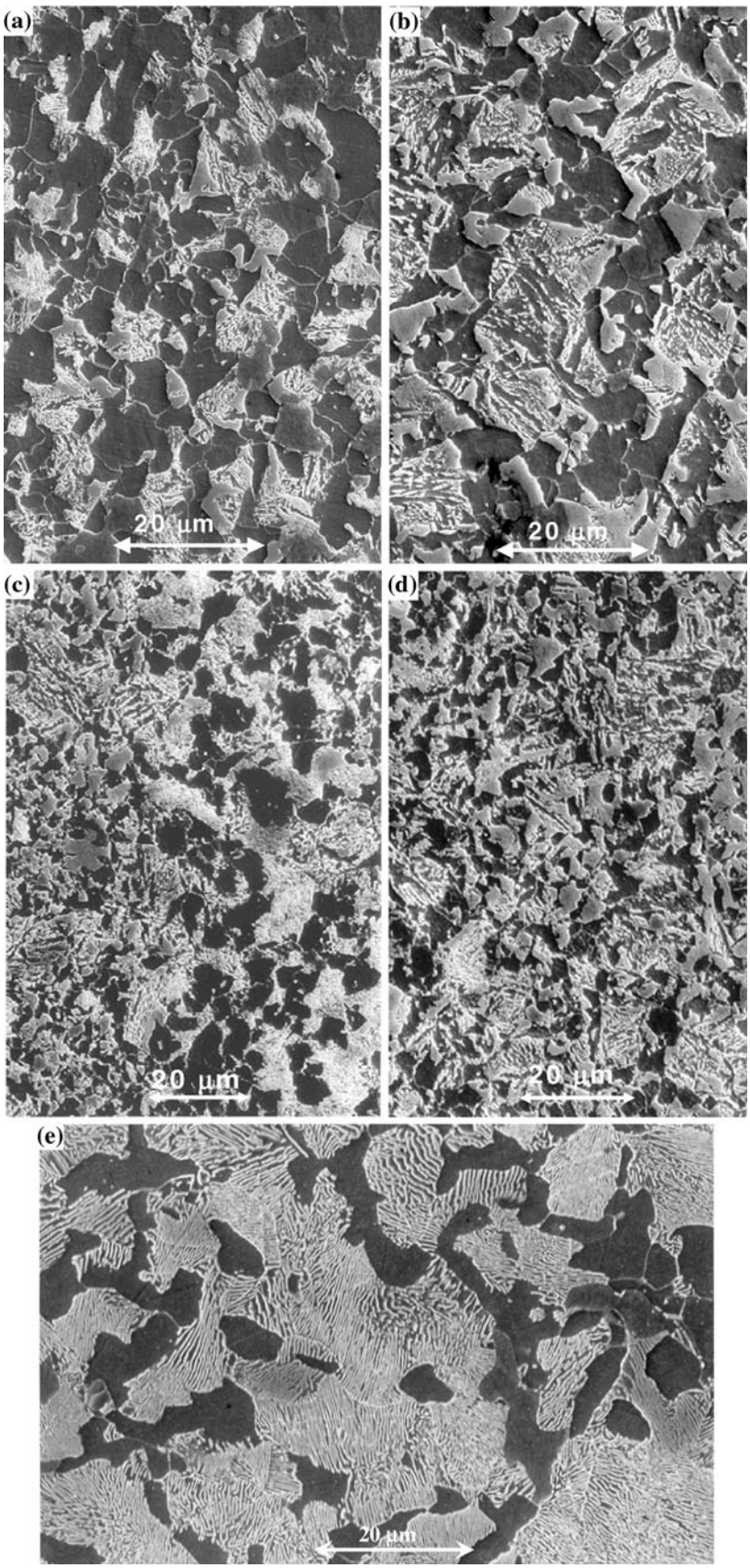

Fig. 2 SEM micrographs of the microstructures generated in: V1 steel after deformation at 870 °C followed by **a** air cooling and **b** accelerated cooling; V2 steel after deformation at 870 °C followed by **c** air cooling and **d** accelerated cooling, and **e** C–Mn steel after deformation at 870 °C followed by air cooling

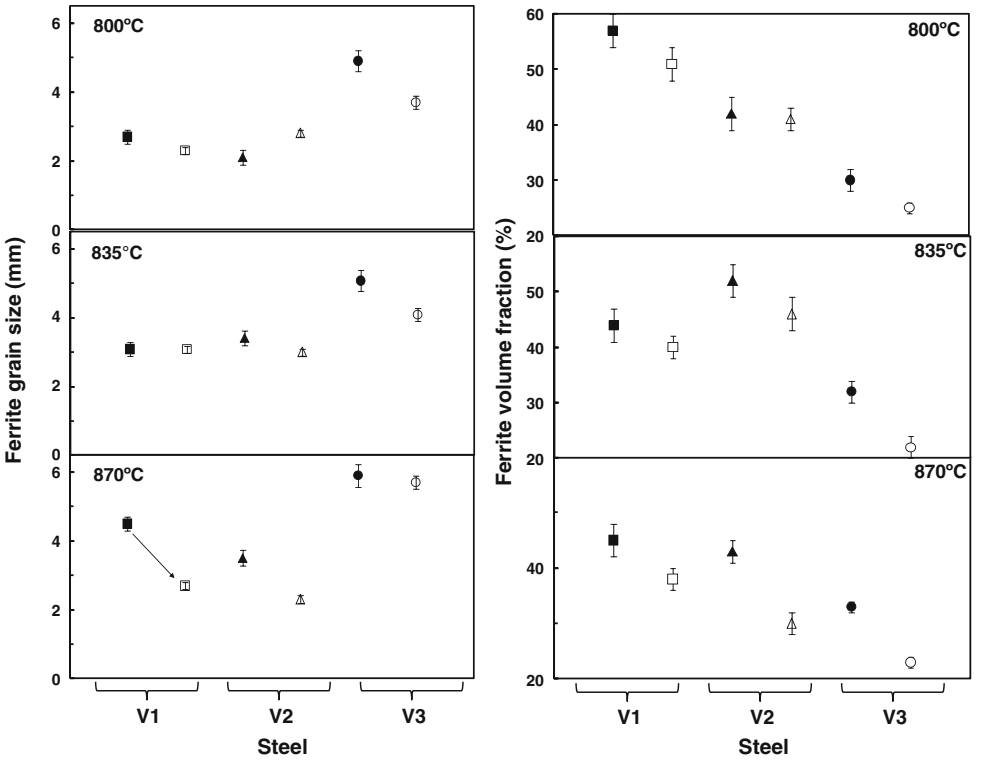

Fig. 3 Ferrite mean grain size and volume fraction as a function of deformation temperature. *Black symbols*: air cooled and *open symbols* accelerated cooled microstructures. *Error bars* indicate the standard deviation

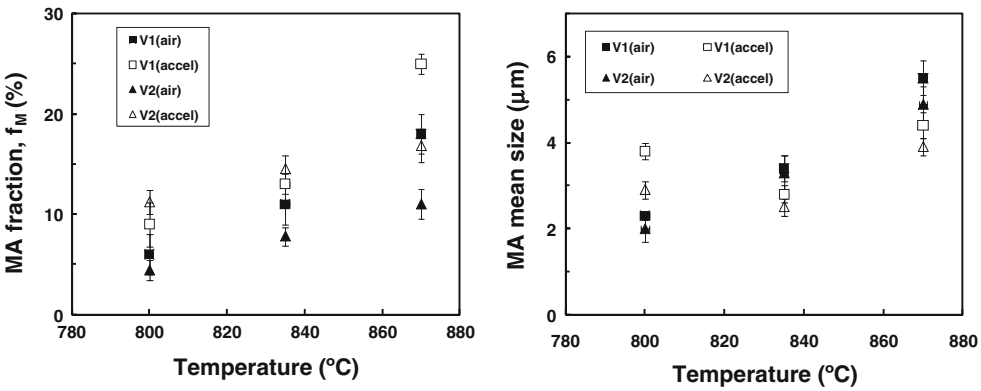

Fig. 4 Evolution of MA volume fraction and mean size as a function of the reheating (deformation) temperature. *Error bars* indicate the standard deviation

has the opposite effect, further details will be given during discussion.

Mechanical properties

In warm forging processes, the flow stress of the steel during deformation is an important factor to evaluate as it affects steel workability and tools wear. The mean flow stress values (MFS) were calculated from the stress–strain curves obtained in the plane strain compression tests. The MFS is defined as the area under the stress–strain curve divided by the applied strain. The values obtained with the three steels are drawn in Fig. 8 as a function of the deformation temperature. As the temperature decreases from 870 to 800 °C there is an increase in the MFS value close to 20% in the three steels and, for a given temperature, the microalloyed steels exhibit higher values than the C–Mn one.

Figure 9 summarises the mechanical properties at room temperature as a function of the deformation temperature (mean values of two samples). In most conditions, the highest yield stress and UTS correspond to the V2 steel, followed by V1 steel. This tendency changes slightly in the samples deformed at 800 °C and accelerated cooled. On the other hand, for a given steel the effect of the deformation temperature does not show a well-defined behaviour. While for the air cooled samples in the V microalloyed steels a slight decrease occurs in the yield stress as the deformation temperature increases, the opposite arises when accelerated cooling is applied. In the case

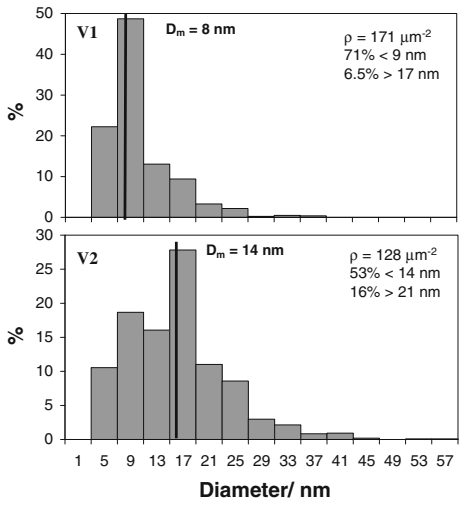

Fig. 5 As received V(C,N) size distribution in V1 and V2 steels. ρ stands for the density of V(C,N) per area unit

of the UTS, for both cooling rates an increasing tendency is observed with higher deformation temperatures. Concerning the C–Mn steel, the influence of the deformation temperature seems to be smaller in both yield stress and UTS values, although a discrepancy is observed in the samples deformed at 870 °C and air cooled.

Another aspect to take into account is that while in all the tensile tests done with the V microalloyed steels over air cooled microstructures the yield curves have a well-defined plateau, in the accelerated cooled conditions this plateau reduces or completely disappears, showing a continuous yielding curve, as the deformation temperature increases.

Ductility, measured as the reduction in area, increases as forging temperature decreases in the V microalloyed steels, showing higher values for the air cooled than for accelerated cooled conditions. Between both V steels, only small differences have been quantified. In contrast, the ductility of the C–Mn steel remains nearly constant independently on the deformation temperature and cooling strategy.

The influence of the deformation temperature on the Charpy curves is shown in Fig. 10. In the case of the V microalloyed steels, the air cooled samples deformed at 870 °C show a remarkable shift of the curves towards higher temperatures, almost 50 °C, compared to the other two deformation conditions. In the case of accelerated cooled specimens, the associated increase in strength is accompanied by impairment of toughness, more notorious in the microstructures corresponding to 830 and 870 °C conditions. Finally, in the case of the plain C–Mn steel the influence of the deformation temperature on the Charpy curves is less important.

Discussion

Microstructures before deformation

The austenite grain coarsening behaviour observed in Fig. 1 may be directly related to the composition of the steels. Grain growth can be influenced by the solute drag effect of any elements in solid solution and by the pinning forces associated to precipitates. The amount of V in solid solution calculated with MTDATA for both V microalloyed steels is

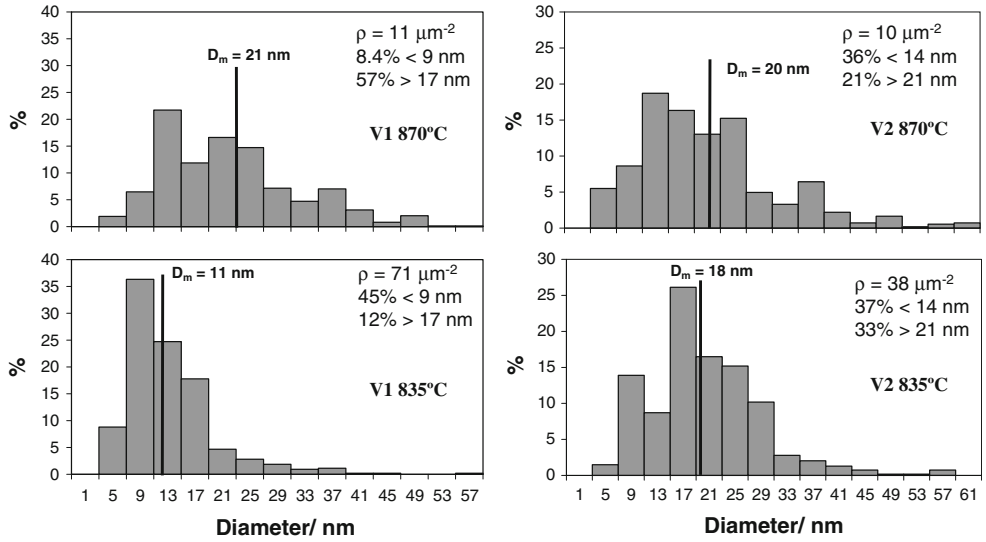

Fig. 6 V(C,N) size distribution in V1 and V2 steels after reheating for 10 min at the indicated temperatures and then water quench. ρ stands for the density of V(C,N) per area unit

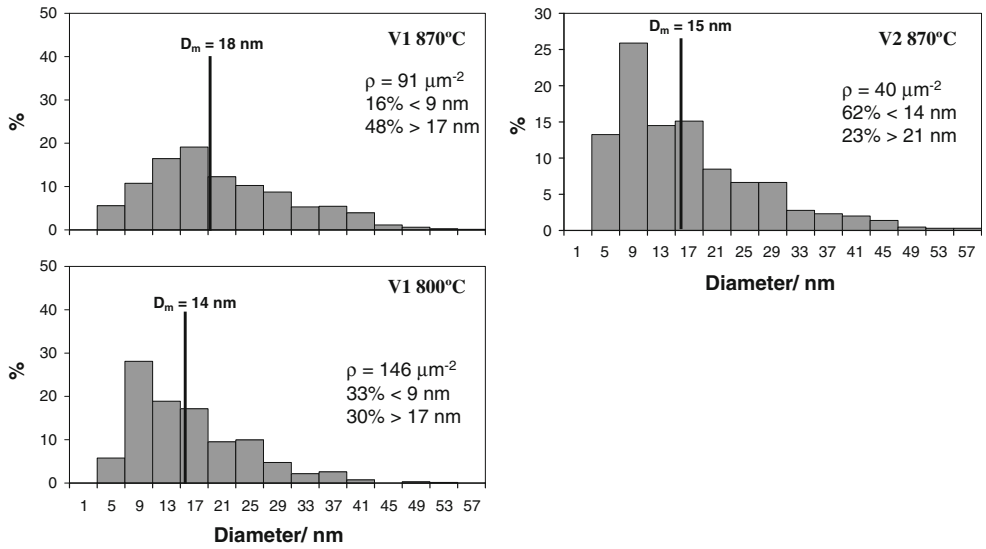

Fig. 7 V(C,N) size distribution in V1 and V2 steels after deformation and air cooling at the specified temperatures. ρ stands for the density of V(C,N) per area unit

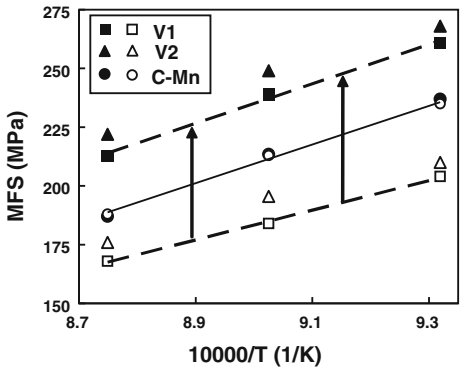

Fig. 8 Mean flow stress (MFS) obtained from plane strain compression tests as a function of deformation temperature (*close symbols*). Experimental results are compared with those predicted by Misaka's modified equation (*open symbols*)

shown in Fig. 11 as a function of temperature. These results indicate that an important fraction of precipitates present in the as received conditions will remain undissolved. Similarly, the size distributions of precipitates measured in the samples quenched after reheating at 835 and 870 °C confirm that they remain very fine and that, in consequence, are able to exert a control in the austenite grain size. As the austenitisation temperature increases and more vanadium is put in solution, grain growth starts over 900 °C but sizes continue being significantly smaller than those measured in the C–Mn steel. This observation agrees with previous results obtained with vanadium microalloyed steels that associate the inhibition of the austenite grain growth with a combined effect of pinning by incompletely dissolved vanadium precipitates and a solute drag effect of vanadium [17].

The other microstructural aspect to take into account before deformation is applied is the situation of V(C,N) precipitates. If the results of particle size distribution after reheating shown in Fig. 6 are compared with those of Fig. 5 (as received condition) it is possible to appreciate that there has been a dissolution process involving, above all, the smallest precipitates. This is supported by data in Refs. [18–20], where it is estimated that the time needed at 870 °C to completely dissolve a vanadium precipitate changes from few minutes for a 6 nm diameter particle to nearly 1 h for a 18 nm diameter one. Although it is not probable due to the moderate reheating temperatures, it could be argued if coarsening of the size distribution is assisted or not by Ostwald ripening. Using Wagner formalism [21], the time required for the coarsening of V precipitates by Ostwald ripening was calculated. The results indicate that a particle of 6 nm needs 1.8 and 7 h to achieve 10 nm at 870 and 835 °C, respectively. This means that coarsening by Ostwald ripening mechanism is very improbable to occur with the applied treatments, thus supporting the idea that the larger size of precipitates after reheating compared to the as received condition may exclusively arise from the dissolution of the smallest particles, as mentioned above.

Finally, and according to the equilibrium calculations shown in Fig. 11, the precipitates present in the as received condition in steel V2 will be more stable than those in steel V1, meaning that their dissolution becomes more difficult. This observation is supported by the fact that in steel V2 an increase in the reheating temperature from 835 to 870 °C implies a 2 nm enlargement in the mean diameter and a drop of about 28 μm^{-2} in the measured precipitate density, ρ, while the same figures for steel V1 are far bigger, 10 nm

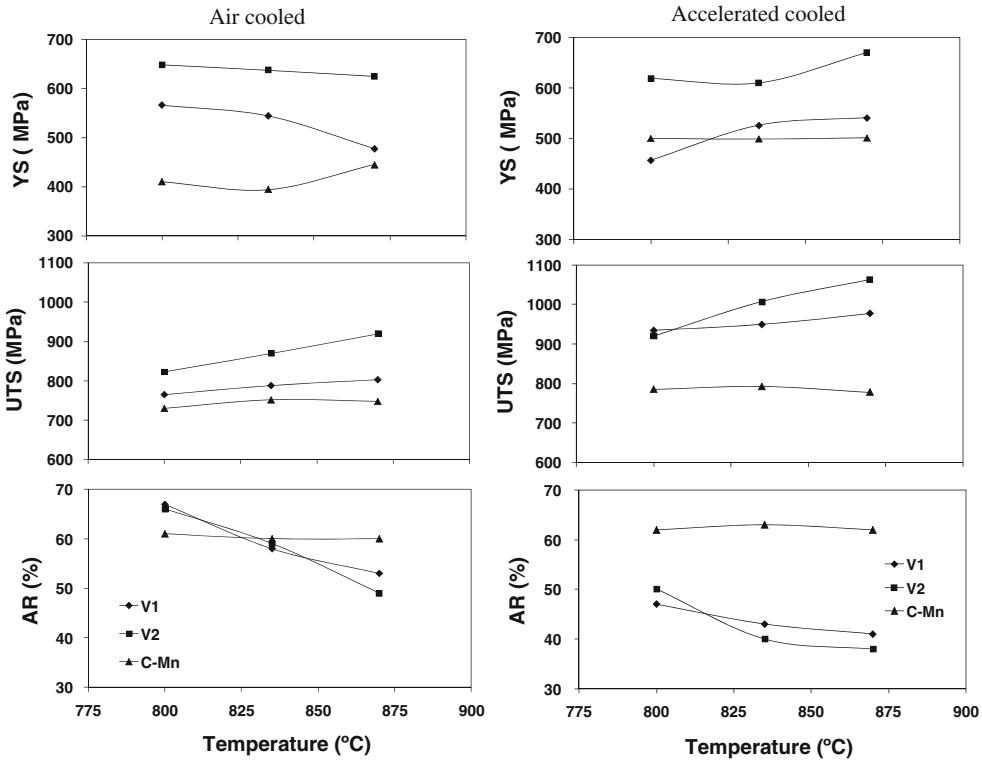

Fig. 9 Mechanical properties as a function of forging temperature

and 60 μm^{-2}, respectively. According with the latter discussion, it is reasonable to assume that at 800 °C, where small dissolution has taken place as predicted in Fig. 11, the size distribution and density of particles must be very close to that of the as received conditions, i.e., higher density of smaller particles as compared to 870 and 835 °C reheating temperatures.

Microstructures after deformation

Figures 3 and 4 indicate that some room temperature microstructural features are very dependent on the deformation temperature in both microalloyed steels. This temperature can interact with the transformation during cooling by modifying two factors: the austenite grain conditioning before transformation and the vanadium dissolution/precipitation situation.

Concerning the austenite microstructure before transformation, in a previous work [14] it was quantified that the presence of undissolved V(C,N) precipitates retards the static recrystallisation process occurring after deformation in the warm temperature regime. This delay becomes longer for lower deformation temperatures. Taking into account the results of the aforementioned work, it can be concluded that in the samples tested at 870 °C, before transformation begins, there will be sufficient time to achieve a completely recrystallisation of austenite. In contrast, at 835 and 800 °C the recrystallisation will be incomplete. This implies that the austenite grain boundary area per unit volume (S_v) before transformation will increase in these last two conditions.

It is well known that higher S_v values favour the microstructure refinement during transformation [22]. This refinement effect is enhanced as the cooling rate is increased. However, it has been reported, in both low and high carbon steels, that as S_v increases the effect of cooling rate to introduce additional refinement becomes weaker [23, 24]. In this context, in both V microalloyed steels the initial austenite grain size prior to deformation is very small. As a consequence, the resulting S_v value in the partially recrystallised microstructures deformed at 800 and 835 °C will be high enough to bring about a very fine ferrite grain size, as shown in Fig. 3, with a minor effect of the cooling strategy. This can explain the behaviour of the ferrite grain size remaining nearly constant in both V microalloyed steels at 800 and 835 °C. In contrast, as at 870 °C the austenite microstructure is completely recrystallised before transformation, S_v will be smaller than in the previous cases, thus leading to some refinement in the ferrite mean grain size when accelerated cooling is applied. In the case of the plain C–Mn steel, a complete recrystallisation of the austenite after deformation [25] and some grain growth could also happen for the three deformation temperatures. As a result, smaller S_v values will be produced, which can explain the slightly coarser ferrite grain size obtained in comparison to the V microalloyed steels.

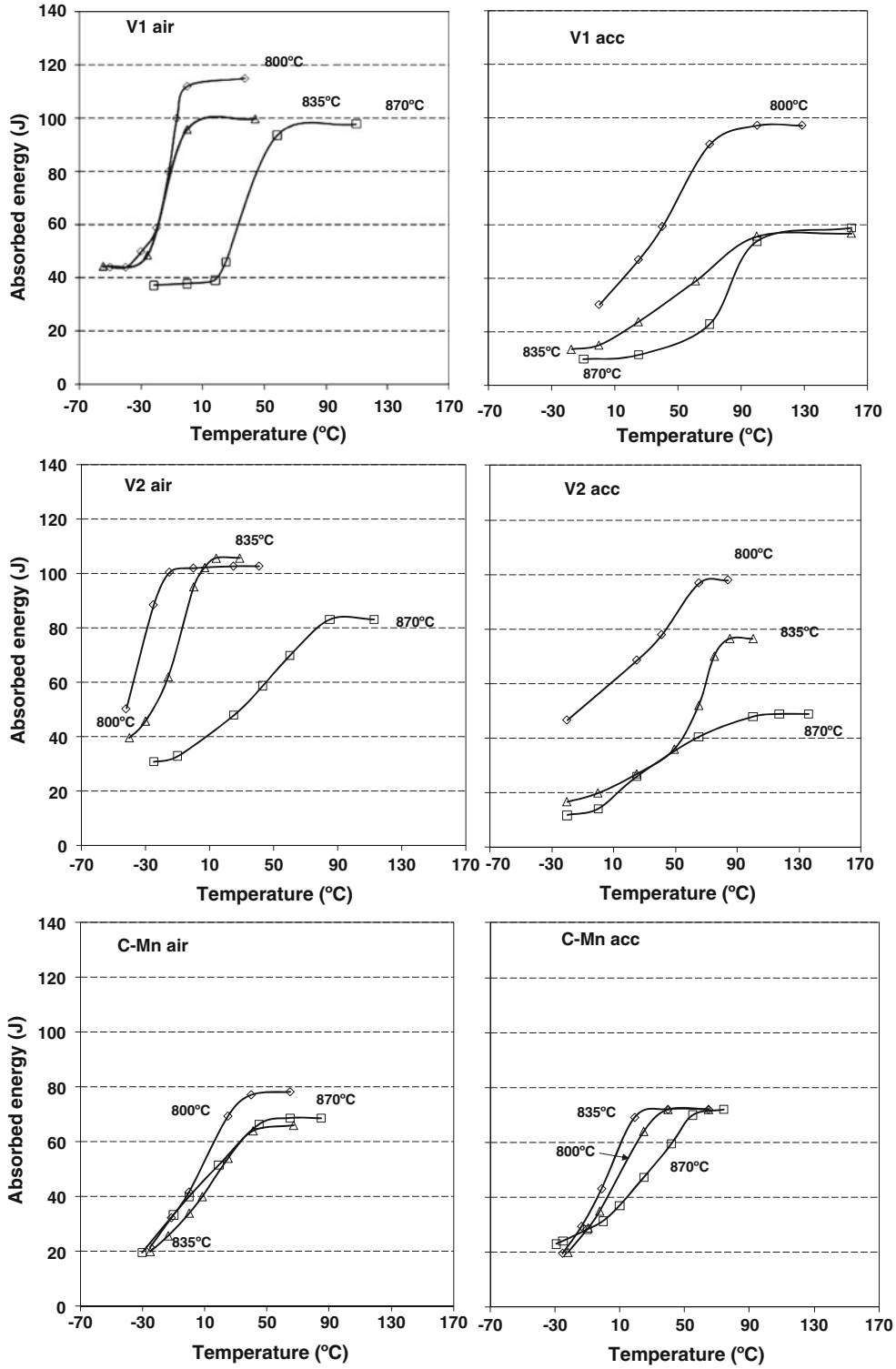

Fig. 10 Charpy test results

The evolution of the ferrite volume fraction with deformation conditions shown in Fig. 3 seems more difficult to explain. Concerning the C–Mn steel, f_α remains nearly independent on the deformation temperature. This can be explained assuming that the possible changes in the austenite grain size between the different deformation conditions are small enough to not affect the CCT curve of the steel. The smaller ferrite fraction resulting at higher

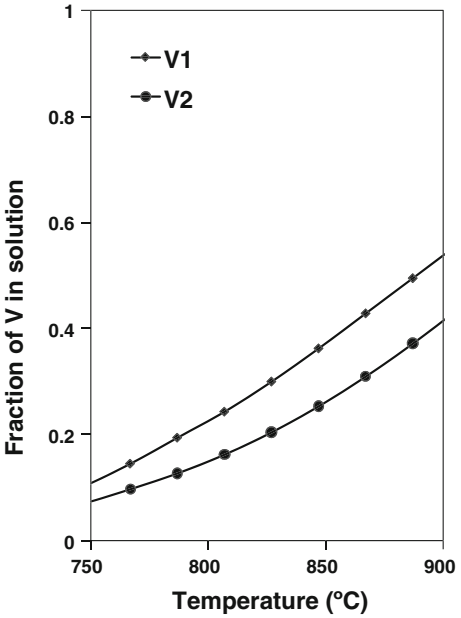

Fig. 11 Theoretical mass fraction of V in solid solution as a function of temperature

cooling rates follows also the expected tendency. In contrast to this behaviour, in both V microalloyed steels some dependence on the deformation temperature is observed.

The dependency of the ferrite fraction with deformation temperature can be considered together with the tendency of increasing MA fraction shown in Fig. 4. Different factors can be interacting simultaneously. Firstly, the accumulated strain in the austenite (at low deformation temperatures) will accelerate the ferrite transformation, i.e., ferrite will start forming at higher temperatures and shorter times, thus favouring higher ferrite fraction contents [24]. Secondly, vanadium in solution delays slightly the start of ferrite transformation and moves the end of pearlite and bainite transformations to longer times [26]. The third factor to take into account is the amount of nitrogen in solution. Staiger et al. identified an important influence of free nitrogen on the increase of the MA microconstituents formation in low C high Mn steels [27]. These authors observed that nitrogen in solution increases the hardenability affecting mainly to those regions where Mn was locally segregated.

These three factors can explain qualitatively the behaviour observed in steel V1, where a decrease in the ferrite and an increase in MA volume fractions occur as deformation temperature increases. In the case of steel V2, the MA fraction evolution follows a similar trend to that observed in steel V1. The lower fractions at 835 and 870 °C, in comparison to those measured in steel V1, could be related to the more stable V(C,N) precipitates (Fig. 11) and, in consequence, to the smaller free nitrogen percentage. In relation to the ferrite volume fraction, while at 800 °C it follows the general behaviour, the increase in f_α measured in the samples deformed at 835 °C, with higher contents than those measured in steel V1 with lower C content, deviate from the expected behaviour. Assuming that the difference in the austenite conditioning in both microalloyed steels at 835 °C is small, the possible role of vanadium remains unclear.

The V(C,N) precipitate size distributions after deformation followed by air cooling shown in Fig. 6 allow one to evaluate the evolution of the amount of vanadium available in solution after reheating. The possibility of strain-induced precipitation in austenite can be ruled out because of the absence of a plateau denoting this effect in the recrystallised fraction versus time plots reported in Ref. [14]. An additional argument for the absence of strain-induced precipitation is that there is no thermodynamic driving force for this to happen since the deformation temperature is the same as the austenitisation temperature Therefore, all the V in solution will be available for further precipitation during cooling, either as new precipitates or on already existing ones.

A higher reheating temperature will lead to an increase in the precipitation rate of new particles through a higher supersaturation during cooling but, on the other hand, lower dissolution temperatures will favour accelerated precipitation of the solutes on pre-existing particles, which act as preferred sites [28, 29]. This is essentially the situation detected in both microalloyed steels. When comparing data of Figs. 6 and 7 for steel V1, it is clear that a refinement in the particle size distribution is attained after deformation applied at 870 °C. The mean size decreases slightly from 21 to 18 nm and there is an important increase in the fraction of particles smaller than 9 nm. This implies that a fine fresh precipitation is taking place during subsequent cooling after deformation, resulting in an important increase in the density of precipitates detected, i.e., from 11 to 91 μm^{-2}. This situation differs from that observed in the samples deformed at 800 °C. Assuming that before deformation the precipitation state at 800 °C should be very similar to that of the as received condition, Fig. 5, there is an increase in the average precipitate size from 8 to 14 nm, in addition to very similar values of ρ and an important increase in the amount of particles bigger than 17 nm. This suggests that the small amount of solute vanadium available is precipitating mainly on pre-existing particles. The behaviour just described for steel V1 is applicable also to steel V2, being the only difference the formation of coarser precipitates for similar deformation conditions.

Mechanical properties

The mean flow stress values can be used for evaluating the forces associated with the warm forging. Several

expressions have been proposed to calculate MFS as a function of composition and deformation parameters. One of these is the Misaka equation (Eq. 1) [30]:

$$\mathrm{MFS(MPa)}9.8\ \exp\left(0.126 - 1.75[\mathrm{C}] + 0.594[\mathrm{C}]^2 + \frac{2851 + 2968[\mathrm{C}] - 1120[\mathrm{C}]^2}{T}\right) \cdot \varepsilon^{0.21}\dot{\varepsilon}^{0.13} \quad (1)$$

where [C] is the carbon content in wt%, T the temperature in K, ε the applied strain and $\dot{\varepsilon}$ the strain rate. As observed, this equation takes only into account the effect of carbon content. Its application to microalloyed grades was done by Kirihata et al. through the introduction of the following multiplying factor that considers the alloy additions [31], all in wt%:

$$f = 0.835 + 0.098[\mathrm{Mn}] + 0.5[\mathrm{Nb}] + 0.128[\mathrm{Cr}]^{0.8} + 0.144[\mathrm{Mo}]^{0.3} + 0.175[\mathrm{V}] + 0.01[\mathrm{Ni}] \quad (2)$$

In Figure 8 the experimental MFS values are compared with the predictions as a function of the absolute inverse temperature, considering Eq. 1 for the C–Mn steel and with the correction of Kirihata et al. for the microalloyed steels, including the vanadium in solution corresponding to each condition in agreement with the predictions of Fig. 11. The results show that there is a good correlation between measured and predicted values for the case of the C–Mn steel, confirming the valuable use of Eq. 1. In contrast, in both microalloyed steels the predictions significantly underestimate the MFS. These differences suggest that other factors, no included in the empirical expressions of Misaka and Kirihata et al., are operating. In this context, it might be suggested that the precipitates present during deformation at the warm reheating temperature range analysed in this study are affecting the flow stress of the steel. It is worth emphasising that Dutta et al. [32] observed that Nb(C,N) precipitates present in austenite lead to a strengthening increment in the flow stress that could be associate directly to the particles. In order to confirm that, an additional plane strain compression test was done at 1025 °C with steel V1. At this temperature it could be considered that all the vanadium is in solution. The MFS value obtained from the flow stress curve was 117 MPa, in very good agreement with the value of 114 MPa calculated from the Misaka–Kirihata equations. This confirms that in warm forging of V microalloyed steels there can be an additional increase in the MFS and, as a consequence, in the forces required to deform the steel, associated to the precipitates present prior to deformation application.

Concerning the room temperature mechanical behaviour, the application of the warm working to the V microalloyed steels has led to multiphase microstructures that made difficult the quantification of the contribution of each

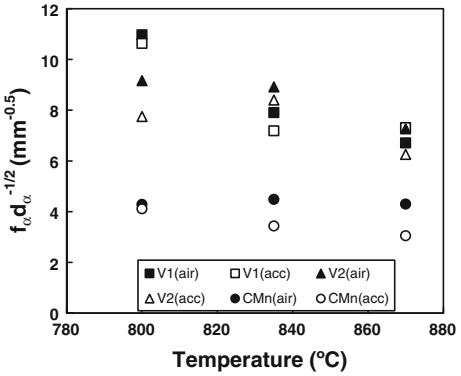

Fig. 12 Evolution of the ferrite phase relevance in the strength, considered through the $f_\alpha d_\alpha^{-0.5}$ factor, as a function of the deformation temperature

hardening mechanism to the overall strength. Nevertheless, there are some general rules that can be taken into account. For example, the influence of the ferrite on the overall strength decreases as higher deformation temperatures are selected in the V microalloyed steels, while it remains nearly constant in the C–Mn steel. This influence has been considered in Fig. 12 through the $f_\alpha d_\alpha^{-0.5}$ product. In the figure, a linear relationship with f_α has been chosen, as this type of dependences between the soft phases and the overall strength have been proposed in the case of multiphase microstructures [33], although for the case of ferrite–pearlite microstructures (that is, the case of the C–Mn steel) the $f_\alpha^{1/3}$ proposed by Gladman et al. is generally accepted [34]. Independently of selecting f_α or $f_\alpha^{1/3}$, the decreasing tendency with deformation temperature shown in Fig. 12 prevails.

The fact that the yield stress and the tensile strength decrease slightly or increase with deformation temperature, depending on the steel and cooling condition, and that the ferrite contribution decreases, implies a higher contribution of other hardening mechanisms, that is, hard constituents as MA (confirmed by the data of Fig. 4), precipitation strengthening and dislocation density (mainly in the accelerated cooled samples). Precipitation hardening evidence has been presented in Ref. [35], where nano-hardness measurements of ferrite were made after different deformation conditions. The results thus obtained showed that ferrite present at the microstructure becomes softer as the deformation temperature and subsequent applied cooling rate decrease. The results are rationalised in terms of the effectiveness of the precipitation strengthening contribution, i.e., precipitate size and distribution. All of these hardening mechanisms will have a deleterious effect on the toughness, measured as ductile–brittle transition temperature.

This toughness deterioration as deformation temperature and cooling rate are increased is confirmed by Fig. 10. As

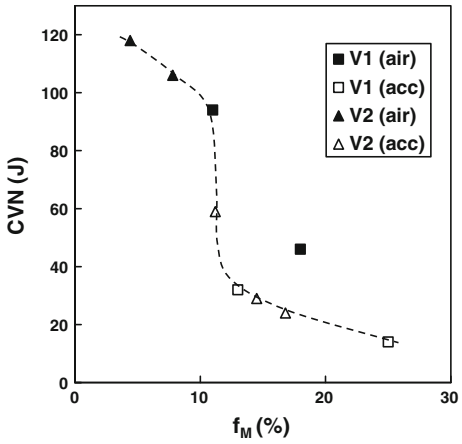

Fig. 13 Dependence of room temperature Charpy energy with hard phase (MA) volume fraction

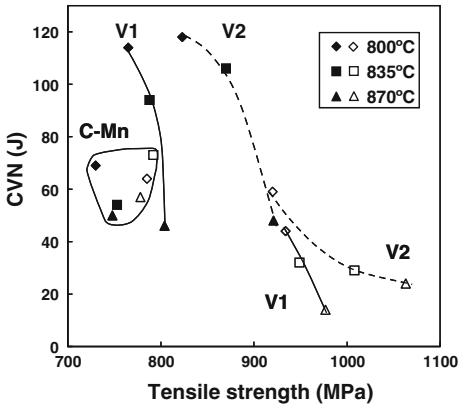

Fig. 14 Relationship between room temperature Charpy energy and tensile strength in air cooled (*closed symbols*) and accelerated cooled (*open symbols*) conditions

mentioned above, these results could be explained in terms of a higher fraction of harder MA constituent (f_M) as deformation temperature and cooling rate are increased [2, 36, 37]. This aspect was also corroborated by further analysis of the fracture surfaces of brittle broken specimens, which showed crack initiation in MA constituents. A similar dependence has been reported in ferrite–martensite microstructures [38]. This deleterious effect of the amount of MA can be observed also in Fig. 13 where the room temperature Charpy energy has been drawn as a function of MA volume fraction. The figure indicates a rapid drop in CVN energy in a small interval of MA fraction: while for MA fractions smaller than $\sim$10% the behaviour corresponds to the complete ductile fracture in both microalloyed steels, once this value is surmounted the absorbed energy abruptly decreases. The different contributions of the microstructural features to the strength and toughness simultaneously can be observed in Fig. 14, where the tensile strength has been drawn against the room temperature Charpy energy. The figure indicates that in the case of the plain C–Mn steel, the different deformation temperatures lead to a reduced strength–toughness window. In contrast, the introduction of V microalloyed steels combined with deformation temperatures between 800 and 835 °C produces an increase in toughness with strength levels similar or higher than those obtained with the C–Mn steel, depending on the amount of V.

When deformation is carried out at 870 °C, the higher amount of V and nitrogen in solution has lead to an increase in the fraction of hard phases that impairs toughness without a significant improvement in strength. The application of higher cooling rates after deformation provides the possibility of obtain higher strength, but at the expenses of a further decrease in toughness. At these conditions it will be possible to achieve higher strength values than those obtained with the plain C–Mn steel, but in spite of a loss in toughness.

Summarising, because of the different amounts of V that are put in solution depending on the applied reheating temperature before warm deformation, it is possible to have important differences in the room temperature microstructure that will affect mechanical properties, showing a higher sensitivity to process parameters than plain C–Mn steels. Taking it into account, in the range of 800–870 °C, the selection of low deformation temperatures should lead to the best strength–toughness combinations. On the other hand, Fig. 8 indicates that microalloying requires higher force tools during forming in comparison to plain C–Mn steels. This aspect should also be taken into account when selecting deformation conditions. Finally, as the loss of toughness is associated with a higher amount of hard phases, similar approaches to those applied to conventional forging, that is, an increase in the Si content of the steel [12, 39] or a reduction in Mn could be considered. This would permit to increase the deformation temperature with the consequent reduction in the requirements of the tool forces.

Conclusions

The main conclusions of this work could be summarised as follows:

- The microstructural and mechanical behaviour of V microalloyed steels show important differences compared to conventional C–Mn steels in warm working processes. These differences arise from the different amounts of V that is put in solution which depends on the applied reheating temperature before warm deformation.

- Given the low temperatures implied in warm forging procedures, i.e., low levels of dissolution and limited coarsening by Ostwald ripening, the size and distribution of the vanadium precipitates in the as received condition are of great importance. These undissolved particles can play different roles depending on the processing temperature: control of the austenite grain growth during reheating, increase of the required tool forces during forming and delay of austenite static recrystallisation after deformation.
- Microalloying with V leads to fine multiphase microstructures formed by ferrite, pearlite/bainite and MA phases. Depending on the reheating temperature, the vanadium in solution will precipitate during cooling as fine particles or precipitate over existing undissolved particles. The amount of each constituent is affected by the reheating temperature.
- At the deformation temperatures of 800–830 °C followed by air cooling both V microalloyed steels results in better strength–toughness combinations compared to the studied C–Mn steel. In contrast, at 870 °C the increase of MA volume fraction significantly reduces the toughness. With accelerated cooling a further increase in strength can be achieved but room temperature impact toughness is markedly reduced.

References

1. Fatemi A, Zoroufi M (2002) Fatigue performance evaluation of forged versus competing process technologies: a comparative study. 24th Forging industry technical conference, Cleveland, Ohio
2. Ghosh SK, Haldar A, Chattopadhyay PP (2009) J Mater Sci 44:580. doi:10.1007/s10853-008-3051-x
3. Tonshoff HK (1982) VDI-Z Integrierte Produktion 124:841
4. Behrens BA, Suchmann P, Schott A (2008) Prod Eng 2:261
5. Reynolds JH, Naylor DJ (1998) Mater Sci Technol 4:586
6. Sheljaskov S (1994) J Mater Proc Technol 46:3
7. Sekiguchi H, Kobatake K, Tokizane M, Osakada K (1988) Development of new thermo-mechanical treatment in warm forging of carbon steel. International conference on physical metallurgy of thermo-mechanical processing of steels and other metals. The Iron and Steel Institute, Japan, p 856
8. Xinbo L, Fubao Z, Jianhua F, Zhiliang Z (2002) J Mater Proc Technol 122:38
9. Yan H, Li Z, Zhang Z (2006) J Zhejiang Univ Sci A 7:1453
10. Zhao P, Boyd JD (2007) Mater Sci Technol 23:1186
11. Xu YB, Yu YM, Xiao BL, Liu ZY, Wang GD (2010) J Mater Sci 45:2580. doi:10.1007/s10853-010-4229-6
12. Korchynsky M, Paules JR (1989) Microalloyed forging steels. A state of the art review, SAE technical papers, no. 890801
13. Adamczyk J, Kalinowska-Ozgowicz E, Ozgowicz W, Wusatowski R (1995) J Mater Proc Technol 53:23
14. Garcia-Mateo C, Lopez B, Rodriguez-Ibabe JM (2001) Mater Sci Eng A 303:216
15. ASTM E 23-1992. Test methods for notched bar impact testing of metallic materials
16. MTDATA (2004) Phase diagram calculation software. National Physical Laboratory, Teddington, UK
17. Elwazzri AM, Wanjara P, Yue S (2006) ISIJ Int 46:1354
18. Rivas AL, Michal GM, Burnett ME, Musolff CF (1996) In: Van Tyne J, Krauss G, Matlock DK (eds) Microalloyed bar and forging steels. TMS, p 159
19. Aldazabal J, Garcia-Mateo C (2005) Mater Sci Forum 500–501:719
20. Aldazabal J, Garcia-Mateo C, Capdevila C (2006) Mater Trans JIM 47:2732
21. Wagner C (1961) Z Electrochemie 65:581
22. Xu YB, Yu YM, Xiao BL, Liu ZY, Wang GD (2009) J Mater Sci 44:3928. doi:10.1007/s10853-009-3526-4
23. Bengochea R, Lopez B, Gutierrez I (1999) ISIJ Int 39:583
24. Jorge-Badiola D, Iza-Mendia A, Rodriguez-Ibabe JM, Lopez B (2010) ISIJ Int 50:546
25. Medina SF, Mancilla JE (1996) ISIJ Int 36:1063
26. Atlas of Continuous Cooling Transformation Diagrams for Vanadium steels by Vanitec, KENT, UK, p 25, 1985
27. Staiger MP, Jessop B, Hodgson PD, Brownrigg A, Davies CHJ (1999) ISIJ Int 39:183
28. Gladman T (1997) The physical metallurgy of microalloyed steels. The Institute of Materials, London, UK
29. Wang HR, Wang W (2009) J Mater Sci 44:591. doi:10.1007/s10853-008-3069-0
30. Misaka Y, Yoshimoto T (1967) J Jpn Soc Technol Plast 8:414
31. Kirihata A, Siciliano F, Maccagno TM, Jonas JJ (1998) ISIJ Int 38:187
32. Dutta B, Valdes E, Sellars CM (1992) Acta Metall Mater 40:653
33. Parker SV, Wadsworth JEJ, Gutierrez I, Rodriguez R, Vandenberghe L, Lotter U (2003) Property models for mixed microstructures. Technical Steel Research, EUR 20880
34. Gladman T, McIvor ID, Pickering FB (1972) J Iron Steel Inst 210:916
35. Garcia-Mateo C, Romero JL, Rodriguez-Ibabe JM (1999) Microstructure and mechanical behaviour of warm forged V microalloyed steels. 41st Mechanical working and steel processing conference, vol XXXVII. Iron and Steel Society, p 653
36. Amer AE, Koo MY, Lee KH, Kim SH, Hong SH (2010) J Mater Sci 45:1248. doi:10.1007/s10853-009-4074-7
37. Lu SP, Wei ST, Li DZ, Li Y (2010) J Mater Sci 45:2390. doi:10.1007/s10853-010-4205-1
38. Mintz B (1997) Metall Mater Trans 28A:2073
39. Ollilainen V, Kasprzak W, Holappa L (2003) J Mater Proc Technol 134:405